`

TITLE:

Miniscope Recording Calcium Signals at Hippocampus of Mice Navigating an Odor Plume.

AUTHORS AND AFFILIATIONS:

Simoes de Souza F. M.1, Williamson R.5, Ma M.1, Teel, A.1, McCullough, C.2, Futia G.2, Crimaldi J. P.4, True A.4, Gibson E.2,3, Restrepo D.1,3

1 Department of Cell and Developmental Biology, University of Colorado Anschutz Medical Campus, Aurora, CO 80045, USA
2 Department of Bioengineering, University of Colorado Anschutz Medical Campus, Aurora, CO 80045, USA,
3 Neuroscience Graduate Program, University of Colorado Anschutz Medical Campus, Aurora, CO 80045, USA
4 Civil, Environmental & Architectural Engineering, University of Colorado, Boulder, CO 80309, USA
5 Neurotechnology Center, University of Colorado Anschutz Medical Campus, Aurora, CO 80045, USA

fabio.simoesdesouza@cuanschutz.edu
diego.restrepo@cuanschutz.edu

...

SUMMARY:

This protocol describes how to investigate the brain-behavior relationship in hippocampal CA1 in mice navigating an odor plume. We provide a step-by-step protocol including the surgery to access imaging of the hippocampus, behavioral training, miniscope GCaMP6f recording and processing of the brain and behavioral data to decode the mouse position from ROI neural activity.

ABSTRACT:

Mice are able to navigate an odor plume with a complex spatiotemporal structure in the dark to find the source of odorants. We developed a protocol to monitor behavior and record Ca^{2+} transients in dorsal CA1 stratum pyramidale neurons at the hippocampus (dCA1) in mice navigating an odor plume in a 50 cm x 50 cm x 25 cm odor arena. Ca^{2+} transients were imaged by an epifluorescence miniscope focused through a GRIN lens on dCA1 neurons expressing the calcium sensor GCaMP6f in Thy1-GCaMP6f mice. We describe the behavioral protocol to train the mice to perform this odor plume navigation task in an automated odor arena. We provide the step-by-step procedure for the surgery for GRIN lens implantation and baseplate placement for imaging GCaMP6f in CA1. We provide information on real time tracking of the mouse position to automate the start of the trials and delivery of a sugar water reward. In addition, we

provide information on the use of an Intan board to synchronize metadata describing the automation of the odor navigation task and frame times for the miniscope and a FLIR camera tracking mouse position. Moreover, we delineate the pipeline used to process GCaMP6f fluorescence movies by motion correction using NorMCorre followed by identification of regions of interest (ROIs) with EXTRACT. Finally, we describe use of artificial neural network (ANN) machine learning to decode spatial paths from CA1 neural ensemble activity to predict mouse navigation of the odor plume.

INTRODUCTION:

Although significant progress has been made in understanding neural circuits involved in olfactory navigation in head-fixed mice[1–3], and in understanding navigation strategies in freely moving mice[4–8] the role of neural circuits in ethologically relevant freely moving navigation of turbulent odor plumes is still unknown. To study whether dorsal CA1 stratum pyramidale neurons at hippocampus (dCA1) sequential neural dynamics play a role in odorant plume navigation, we monitored neural activity by imaging Ca^{2+} transients in cells expressing the genetically encoded calcium sensor GCaMP6f in Thy1-GCaMP6f mice[9]. We imaged GCaMP6f fluorescence through a miniature epifluorescence microscope focused through a GRIN lens on dCA1[10–12] . We monitored simultaneously spatial navigation and dCA1 neuron GCaMP6f calcium transients in mice performing an odor-plume navigation task where they received a water reward when they reached the spout delivering an odorant into an odor arena with a background laminar air flow[13, 14]. In this article, we describe the methods required to achieve this task (Figure 1), including the stereotaxic surgery for the implantation of GRIN lenses, the placement of a baseplate to secure the miniscope to the skull in a freely moving mouse, imaging with the miniature microscope and monitoring mouse movement with a high-speed FLIR camera, the data pre-processing for removing motion artifacts and finding the regions of interest (ROIs), and the preparation of datasets and artificial neural network training and prediction for decoding the X and Y positions of the mouse in the odor arena from the dCA1 ROIs[7].

Our findings indicate that it is possible to decode the trajectory of the mouse navigating an odor plume based on neuronal ensemble calcium signals in dCA1. Understanding the role of dCA1 calcium signals in odor plume navigation is a crucial step to crack the neural circuit basis for odor-guided navigation in realistic environments[13, 14].

PROTOCOL:

Studies were carried out in 3-to-6-month-old male and female Thy1-GCaMP6f transgenic mice[15]. All experimental protocols were approved by the Institutional Animal Care and Use Committee of the University of Colorado Anschutz Medical Campus, in accordance to National Institutes of Health guidelines. The surgical procedures for GRIN lens implantation (Protocol 1) and the baseplace placement (Protocol 2) were adapted from previous works[16–18].

1. Stereotaxic surgery for implanting a GRIN lens implantation in the hippocampus.

1.1 The surgeon wears sterile gloves, a headcover, surgical mask and a lab coat.

1.2 Sterilize all surgical equipment by autoclaving

1.3 Place sterile drapes around the surgical area

1.4 Anesthetize the mouse by placing it in the induction chamber with 3% isoflurane for 10 min.

1.5 Check whether the mouse stops moving and is under deep anesthesia confirmed by pinching the hind paw to test the hind paw reflex.

1.6 Switch the isoflurane flow to the nose cone.

1.7 Make sure the isoflurane SomnoSuite (Jove Materials Spreadsheet) has the temperature pad set to homeothermic settings and make sure the vapor source is set to external compressed.

1.8 Place the anesthetized mouse in the Stoelting stereotaxic-Digital Manipulator Arm, 3-Axes, Add-On, LEFT (Stoelting, Jove Materials Spreadsheet). Place the front teeth of the mouse into the bite bar and place the nose cone in front of the nose to ensure the isoflurane flow and to lock the head into place. Adjust the level of anesthesia to between 2 to 3% according to the paw reflex after pinching (Figure 2 A).

1.9 Place the mouse ear bars into the ears and tighten. Ensure the mouse's head is horizontal and does not move side-to-side or up and down. When the head is secure, lightly pressing downward on the skull shouldn't cause the skull to slip out underneath the headbars.

1.10 Place the temperature probe in the rectum and tape the wire on the mouse's tail to avoid movement. Set the temperature of the pad to maintain the rectal temperature at 37 degrees Celsius.

1.11 Add ophthalmic ointment to the eyes to prevent harmful air drying.

1.12 The hair is shaved when head is fixed and under the isoflurane flow provided by the nose cone to prevent movement. Shave the hair above the head with an electric shaver, then clear any remaining hairs off with nair and sterile q tip (Figure 2 B).

1.13 Make the operating field sterile by swabbing the scalp with a sterile q tip with ethanol and betadine three times each.

1.14 Inject 0.1 mL of the local anesthetic lidocane under the skin between the eyes and ears. This will make a bubble. Wait for a few minutes before cutting the skin with a scissors.

1.15 Using a tips only technique, pull the skin up carefully using forceps and use a pair of small scissors to remove a circular portion of the skin. Absorb any blood with a sterile cotton swab.

1.16 Once the bleeding stops, clean the skull with hydrogen peroxide (5%) using a sterile cotton swab. Bone landmarks, including where the sagittal suture and the bregmatic suture intersect to mark bregma should be easy to identify after this procedure.

1.17 Attach a pipette to the micromanipulator holding a needle to apply tattoo ink. Make a mark on the top of Bregma.

1.18 Zero the micromanipulator coordinates on Bregma and move to the coordinate above CA1 in the right hippocampus (medium-lateral +1.8mm from Bregma, anterio-posterior -2.4mm from Bregma)[2]. Carefully drill a small permanent dent of 1 mm diameter with a drill at speed of 10K min^{-1}-(Osada, Jove Materials Spreadsheet) to make a permanent dent on the top of the target location (Figure 2 C).

1.19 Use the dental drill to open a circular perforation of 1.5 mm diameter to allow the implantation of a 1 mm diameter and 4 mm length GRIN lens into the Brain (Inscopix, Jove

Materials Spreadsheet) (Figure 2 D).
1.20 Puncture the dura and cortex by inserting a 23 gauge needle in the middle of the hole and move the needle into the brain slowly (~0.1 mm/min) until it reaches the depth of 1.25 mm below dura. Remove the needle slowly from the brain (~0.1 mm/min). Use sterile cotton swabs and saline to clean the blood.
1.21 We used a custom made UCLA's GRIN lens holder constructed with two 1ml micropipette tips cut to fit inside each other (GRIN lens holder, Jove Materials Spreadsheet) (Figure 2 E, F). Connect the GRIN lens holder on the micromanipulator and turn on the aspirator connected to the pipette to hold the GRIN lens. Implant the GRIN lens slowly into the cortex until reaches the depth of -1.25 mm below dura.
1.22 Place a drop of liquid tissue adhesive 3M Vetbond (Vetbond, Jove Materials Spreadsheet) into the circular cranium perforation to seal the hole. Wait a few minutes to dry.
1.23 Prepare quick adhesive cement -biocompatible methacrylate resin- C & B Metabond (Metabond, Jove Materials Spreadsheet) on the base of the GRIN lens to permanently seal it on the skull. Wait a few minutes and let it dry.
1.24 Turn off the aspirator to release and slowly remove the GRIN lens holder from the top of the GRIN lens that at this point is permanently attached to the skull.
1.25 Place the head bar on the top of the skull centering the hole on the GRIN lens (Figure 2 G, H, I).
1.26 Carefully place quick drying Metabond adhesive cement (Metabond, Jove Materials Spreadsheet) around the base of the GRIN lens to seal the cranial window and attach the head bar to the skull. Place drying C&B Metabond adhesive cement (Metabond, Jove Materials Spreadsheet) in the middle of the head bar and on the sides, to keep it tightly fixed on the skull. Make sure it is completely dry. Ensure that no adhesive cement is placed on top of the GRIN lens otherwise it will permanently degrade the optical path and block the image.
1.27 Place a drop of low toxicity silicone adhesive (Kwik-sil, Jove Materials Spreadsheet) on top of the GRIN lens for protection from physical damage.
1.28 Turn off the Isoflurane
1.29 Inject buprenorphine SR subcutaneously 0.001 mg/g immediately after surgery for analgesia.
1.30 Take immediate post-operative care monitoring until the animal wakes from anesthesia. Post-operative care is taken until the fully recovery from the surgery by monitoring the mice for signs of pain. Briefly, movement around the cage, eating and drinking and normal reaction to handling is used to ensure that they are not under pain or stress. If the animals show signs of severe neurological or tissue damage, which was out of the ordinary for the procedure, they will be humanely euthanized immediately.

2. Baseplate placement for the miniscope
You can start imaging dCA1 one week after the surgery, after the animal fully recovers.
A baseplate is fixed on top of the GRIN lens for optical access of dCA1 GCaMP6f fluorescence through the GRIN lens using a miniscope. In this protocol, we used the miniscope version 4 -V4 (Miniscope V4, LabMaker, Jove Materials Spreadsheet).
2.1 Two to three weeks after surgery start head-fixing the mouse for 10 min by securing the head bar with pinch clamps for acclimating the mouse to being head fixed.

2.2 Head-fix the mouse four weeks after the surgery and attach a miniscope to a holder attached to a micromanipulator (Sutter micromanipulator, Jove Materials Spreadsheet).
2.3 Place the miniscope in a 3D printed holder (Miniscope Holder, Jove Materials Spreadsheet) attached in a micromanipulator (Figure 3A, B).
2.4 Carefully remove the silicone adhesive (Kwik-sil, Jove Materials Spreadsheet) from the top of the lens using fine tweezers and clean the surface of the GRIN lens using a Zeiss lens wipe.
2.5 Secure the baseplate attached to the miniscope tightening the set screw on the side of the baseplate (Miniscope baseplate V2, Jove Materials Spreadsheet) (Figure 3 C, D).
2.6 Move end of the miniscope until reaching 100 um above the GRIN lens. Use the Miniscope software (Miniscope DAQ-QT Software, Jove Materials Spreadsheet) to view the top of the GRIN lens. Keep the power low, around 10%, and use an acquisition rate of 10 Hz. You should be able to see the circular shape of the GRIN lens on the screen.
2.7 Control imaging of the v4 miniscope using the Miniscope Software (Miniscope DAQ-QT Software, Jove Materials Spreadsheet). Use the sliders in the software to control the power (keep it around 10%) and set the acquisition rate around 10 Hz.
The v4 miniscope has an electrowetting lens that can be used for fine focusing. Place the electro-wetting-lens in the middle of the focal range.
2.8 Bring the miniscope closer to the GRIN lens by adjusting the axial position with the Sutter micromanipulator and monitor the image with the computer. Once you are able to image the top of the GRIN lens, use fine focus up and down on the Sutter micromanipulator to reach the best focal plane to visualize cell flashes. Use the pseudo dF/F setting in the miniscope software to double check the quality of the cell flashes. You should set the focus to the maximum number of cells in the field of view with highest attainable fluorescence intensity. At this point blood vessels should be in focus.
2.9 Once you optimize the focus, carefully build a wall of quick adhesive cement between the skull and the bottom of the baseplate. Take care not to cement the miniscope on the baseplate and be very careful not to get any cement on the top of the GRIN lens.
2.10 Once the cement is dry, remove the set screw and carefully remove the miniscope from the baseplate with the micromanipulator.
2.11 Use the base plate cover to protect the GRIN lens.

3. Construction of the Odor Arena
We constructed an automated odor arena based on the design of Connor et al.[13] and Gumaste et al.[14]. The complete assembly can be found here (Odor Arena Hardware, Jove Materials Spreadsheet).
3.1 The chamber dimensions are 50 cm (L) x 50 cm (W) x 25 cm (H) with 2 acrylic walls, an acrylic ceiling, a white expanded PVC floor, and 2 unique walls at the front and rear which facilitate air flow (Figure 4A).
3.2 The air suction end at the rear of the arena has a tapered design with a computer fan attached to draw air out of the chamber. A physical knob sets the fan PWM to regulate the rate of air flow. A 3D printed honeycomb structure comprises walls for the front and rear of the odor arena to facilitate laminar flow of air while retaining a mouse inside [10]. The honeycomb wall at the front of the arena has an external flare for receiving large volumes of air in a non-disruptive manner.

3.3 The water reward is delivered via simple contraptions having a Nema 17 stepper motor coupled to a syringe. An A4988 microstepping driver allows precise control of the dispensed volume (https://github.com/dougollerenshaw/syringe_pump, Figure 4B).

3.4 The air intake end has 4 sets of odor sources paired with water-delivery spouts, with each set positioned 10 cm apart along the x axis to define the 'lanes' along which an animal will navigate for a water reward (Figure 4C, D).

3.5 Odor delivery is managed by a system of solenoid valves connected to tubes and odorant bottles (Figure 4D). The valves are powered using a relay board in an arrangement which guarantees that either clean air or odorized air is flowing at all times, and that either one single lane or zero lanes can receive odorized air at any given time.

3.6 Animal behavior is monitored at 60 Hz using a single FLIR Blackfly S camera mounted above the arena (FLIR Camera, Jove Materials Spreadsheet). A 3.5mm fixed focal length C-Series lens was mounted via a C/CS mount adapter, capable of capturing the entire arena (Focal Lens, Jove Materials Spreadsheet).

3.7 The odor arena hardware is managed using custom software developed in Python. A PC connected to a Teensy 4.0 development board provides the means for computer-mediated odor and water delivery. The software integrates the camera and all hardware necessary for setting up experimental parameters and acquiring experimental data (Odor Arena Software, Jove Materials Spreadsheet).

3.8 The FLIR camera exports a clock signal when recording video frames. The signal is used for post-hoc synchronization with the Miniscope using an Intan Board which records the sync out signals from both systems. During an experiment, the custom acquisition software also creates an events file which contains the important experimental events and the camera frame on which the event occurred. A timestamps file is also created to identify any dropped frames, a rare event.

4. Air speed of the plume measured with a photo-ionization detector (Figure 5A)

4.1 Place a fast response miniature PID at two different distances. One location is close and another location far -10 cm apart- from the odor source.

4.2 Turn on the odor valve.

4.3 Measure the delay to detect the odor plume at each location.

4.4 Divide the difference of the delays in each location by the difference of the distance to calculate the air speed of the plume.

5. Behavioral training mouse in the Odor Arena.

We used a behavioral task adapted from Findley et al.[4]. The mouse is water restricted the day before to motivate seeking a water reward. The mouse navigates the odor plume (Figure 6B) towards a water spout located at the source of odor release to obtain water reinforcement (3 drops of 10 µL delivered at 1Hz). During the training period the mouse is maintained under the water restriction by having access to up to 2 mL a day. The body weight of the mouse is monitored during the water restriction period and should not be bellow 85% of the original body weight. The mouse receives approximately 1 mL of water per day during the training in the odor arena and is supplemented with an additional 1 mL of water per day in the cage after training. The mouse stays under water restriction for a maximum period of 72 hours.

5.1 First, train the mouse to start trials by moving to the back of the arena (defined as the portion of the arena that is 40 cm away from the side where the air flows into the chamber). Wait the mouse goes to the back of the arena and then manually deliver odor and water in one random lane and let the mouse find the source and drink the water. Repeat the procedure many times to create the association between odor and water (Figure 6A, B). Once the mouse learns to start trials, then use the automated software to deliver odors.
5.2 Then train the mouse to do the two-lane odor navigation task. In this task one of two odor ports is randomly chosen to deliver odor and the mouse is reinforced with water when it arrives to the water spout where odorant is delivered. We used the odorant Isoamyl Acetate diluted at 1% in mineral oil.
5.3 The mouse completes a session of about 20 trials of odor plume navigation in about 40 min. The trained mouse achieves a percent of correct navigation above random choice in the end of the session (> 65% correct choices).

6. Epifluorescence recording of a freely moving mouse in the odor arena

We recorded neuronal activity of stratum pyramidale (SP) cells in dorsal CA1 by imaging the genetically encoded calcium sensor GCaMP6f expressed in Thy1 mice [9] by wide field miniscope imaging during the two spout odor plume navigation task (Supplementary Movie 1, 2).
6.1 Head fix the mouse, place the miniscope on the top of the baseplate using the Sutter micromanipulator and tighten the set screw.
6.2 Adjust the electrowetting lens to find the optimal focal plane with the largest number of cells with highest fluorescence intensity.
6.3 Adjust the miniscope power to obtain the optimal dynamic range with a high signal to noise ratio without saturation. This is usually attained imaging dorsal CA1 in Thy1-GCaMP6f mice with miniscope power set around 30% at an acquisition rate of 30Hz.
6.3 Release the mouse inside of the odor arena with the miniscope attached to the baseplate.
6.4 Start acquisition with the Intan board to record the TTL output of the FLIR camera located at the top of the arena and the TTL signal from the miniscope for latter synchronization between behavioral and GCaMP6f video frames. The FLIR camera records at 60 Hz and the miniscope records at 30 Hz.
6.5 Start recording the miniscope and behavioral movies and turn on the automated software for two spout odor navigation task.

7. Data Preprocessing

We used a MATLAB pipeline to process the data (Figure 7). The code is deposited in GitHub (Synchronization Software, Jove Materials Spreadsheet). NoRMCorre[19] was used for motion correction and EXTRACT[20] to find the ROIs with time-varying fluorescence signals reported as changes in fluorescence normalized by fluorescence between calcium transients ($\delta F/F$).
7.1 Synchronize the odor arena metadata, the FLIR frames and the miniscope frames using the sync signals recorded by the Intan board by running the matlab code Synchronize_Files_JOVE.m available on Github (Synchronization Software, Jove Materials Spreadsheet).
7.2 Perform motion correction of the synchronized miniscope frames using NoRMCorre (Motion Correction Software, Jove Materials Spreadsheet).
7.3 Find the ROIs with time-varying $\delta F/F$ signals using EXTRACT (ROI Extraction Software, Jove

Materials Spreadsheet).
7.4 Separate the data into trials.
7.5 Label each trial either as a hit or a miss based respectively on the mouse's correct or wrong navigation behavior.
7.6 Use Behavior Ensemble and Neural Trajectory Observatory (BENTO)[21] to visualize the behavior and ROIs of each separate trial (Figure 8 A, B, Supplementary Movie 4).

8. Data Analysis – Decoding Spatial Position from Brain Signals
We used machine learning to decode the X and Y positions of the mouse in the arena from the dCA1 ROIs[7]. The MATLAB code is available (Decoding Brain Signals Software, Jove Materials Spreadsheet) in https://github.com/restrepd/drgMiniscope.
8.1 The software drgDecodeOdorArenav2.m takes as input the EXTRACT.mat output file and the odor arena metadata file. In the GitHub repository we provide these two files for an example (Synchronization Software, Jove Materials Spreadsheet):

```
dFF_file='20220804_FCM22_withodor_miniscope_sync_L1andL4_ncorre_ext.mat';
arena_file='20220804_FCM22withodor_odorarena_L1andL4_sync.mat';
```

8.2 drgDecodeOdorArenav2.m creates a dataset divided by within trial data containing the ROI signals and metadata (X and Y positions of the mouse, odor spout location, water delivery, etc) for each trial. The code also analyzes decoding for data between trials.
8.3 The code uses fitrnet to train an artificial neural network with the dF/F data for all ROIs for all trials but one to predict x and y positions and predict the position of the trial left out using a leave one out procedure.
8.4 The neural network returns the X and Y positions as output. Use the trained neural network to make predictions. Input left out trials not used to train the network to make predictions of the X and Y positions of the mouse in the arena from the ROIs (Figure 9A, B).

REPRESENTATIVE RESULTS:
Following the use of this method, you should be able to visualize and record dCA1 GCaMP6f fluorescence transients in mice navigating the odor arena to find the source of odorants (Figure 6 A,B, Supplementary Movie 1, 2). The fluorescence images are then motion corrected with NoRMCorre and ROIs are extracted with EXTRACT (Figure 7). In addition, recording with an Intan allows to synchronize the δF/F signals from the ROIs with odor and water delivery events in the odor arena (Figure 8A), as well as with movement of the mouse in the odor arena (Figure 8B, Supplementary Movie 3).

Furthermore, the protocol yields decoding of the X and Y positions of the mouse from the δF/F signals of the dCA1 ROIs (Figure 9). Decoding the trajectory of the mouse from neuronal ensemble calcium signals in dCA1 is significant because it reveals how neurons in dorsal CA1 represent a cognitive map of odorant and spatial information to perform the complex task of odor plume navigation. We are in the process of differentiating ROIs that behave exclusively as place cells and other cells that respond to the odor stimulus. Successful decoding of the

trajectory of the mouse from neuronal ensemble signals can be confirmed by the strong correlation between the decoding prediction and the ground true X and Y positions of the mouse.

FIGURE AND TABLE LEGENDS:

Figure 1. Study Pipeline.

A: The stereotaxic surgery consists of implanting a GRIN lens in the CA1 layer of hippocampus and a headplate on the skull for head fixing the mouse. B: A baseplate is placed on the top of the GRIN lens to allow accessing optically the fluorescence of the CA1 neurons with a miniscope. C: The mouse is trained on the odor plume navigation task. D: Freely moving recording of the mouse behavior and CA1 neurons navigating the odor plume.

Figure 2: Stereotaxic Surgery.

A: Place the anesthetized mouse in the stereotaxic apparatus. Adjust the level of anesthesia between 2 to 3% accordingly with the pinching paw reflex response

B: Shave the hair above the head.

C: Carefully drill a small permanent dent with drill to make a permanent dent on the top of the target location.

D: Use the dental drill to open a circular perforation of 1.5 mm diameter to allow the implantation of a 1 mm diameter and 4 mm length GRIN lens into the Brain.

E: Connect the GRIN lens holder on the micromanipulator and turn on the aspirator connected to the pipette to hold the GRIN lens.

F: Implant the GRIN lens slowly into the cortex until reaches the depth of -1.25 mm below dura matter.

G: Illustrative post-mortem fixed head showing the head-plate and base-plate cemented on the skull with the implanted GRIN lens.

H: Post-mortem CT-scan of the head illustrating the Head Bar on the top of the cranium and the GRIN lens implanted inside of the cranium.

I: Design of the head-plate to yield head-fixing the mouse.

Figure 3: Miniscope base plate placement.

A: 3D printed miniscope holder coupled to a Sutter MP-285 micromanipulator.

B: Miniscope attached to the holder. C: Attaching the baseplate to the miniscope. D: Tightening the set screw for fixing the baseplate to the miniscope. The set screw is released after cementing the baseplate to the mouse skull.

Figure 4. Construction of the Odor Arena.

A: Odor arena transparent Chamber. There is a top FLIR camera for recording the mouse behavior. B: Step motors coupled to syringes control the water delivery to reward the mouse. C: View from the inside of the odor arena showing a honeycomb structure is used to yield a laminar flow and four odor delivery lines. D: Odor delivery system including tubes, valves and odor bottles viewed from the outside of the odor arena.

Figure 5. Odor plume recording.
A: Odor plume recorded with the photoionization detector (PID). Mean(bold blue)±Standard Deviation (light blue) of five PID traces of an odor plume propagating at 4.23 cm/s in the odor arena. Odorant source at 2cm from the odor arena floor. B: Laser recording of the odor plume with unbounded flow at 20 cm/s.

Figure 6. Mouse Behavioral Training.
A: Mouse learning to navigate toward an odor plume released on the right lane. The mouse learns to start a trial by going to the back of the odor arena, decide a side to navigate toward the odor plume, and drink a water reward. B: Mouse learning to navigate toward an odor plume released on the left lane. The mouse is rewarded with odor if navigating to the correct lane.

Figure 7. Data Analysis Pipeline
A: The data from the odor arena and miniscope are synchronized (Synchronization Software, Jove Materials Spreadsheet). B: Motion correction is performed by NoRMCorre (Motion Correction Software, Jove Materials Spreadsheet). C: The ROIs are extracted with EXTRACT (ROI Extraction Software, Jove Materials Spreadsheet). D: The $\delta F/F$ signals of the ROIs and the synchronized behavioral frames are visualized with BENTO. E: The X and Y position of the mouse is decoded from the ROIs (Decoding Brain Signals Software, Jove Materials Spreadsheet).

Figure 8. Pre-Processing the Data
A: Calcium traces synchronized with the odor arena events for many trials. Each single trial starts with the odor delivery in red and the rewarded trials end with a water delivery pulse in blue. The calcium traces for each ROI are shown in black. An Intan board is used for recording the TTL outputs of the top camera on the odor arena and the miniscope camera for synchronizing the frames. Normcorr is used for correcting the movement noise from the miniscope frames and Extract is used to find the ROIs and extract the dF/F calcium traces. B: Representative example of a single trial. The simultaneous visualization of the synchronized behavior and calcium traces from each ROI of a single trial are observed with BENTO.

Figure 9. Decoding the position of the mouse from the CA1 signals.
Decoding the X and Y position of the mouse from the CA1 ROIs. The decoding prediction is shown in blue and the mouse ground true position is shown in red. The predicted traces are strongly correlated with the ground truth.
A: Decoding the X positions from the ROIs (Pearson Correlation Coefficient = 0.88). B: Decoding the Y positions from the ROIs (Pearson Correlation Coefficient = 0.88).

DISCUSSION:

In this protocol, we described the steps to record place-cells and odor-responsive cells in the dCA1 area of the hippocampus of mice navigating an odor plume. The critical steps in the protocol include stereotaxic surgery, placement of the miniscope baseplate, construction of the odor area, checking the plume in the odor arena, behavioral training, miniscope recording of the freely moving mouse, data pre-processing, and data analysis. Additionally, we explained the

protocol for decoding the mouse trajectory from the dCA1 recordings.

A critical step in stereotaxic surgery is to follow the coordinates relative to Bregma to place the GRIN lens at the correct location. A limitation of the method is the delay between the surgery and the time to start observing GCaMP6f signals, which takes two to four weeks. The mouse should be ready for use after this critical period. Another limitation is the optical aberration of the GRIN lens, which limits the field of view. A crucial step for the baseplate placement is to keep the electrowetting lens at the center to prevent a limitation inadjusting the Z plate after cementing the baseplate on the head. A limitation of the construction of the odor arena is the system's complexity, which can take several months and may require the assistance of an engineer. A limitation of the behavioral training is that mice may prefer one side of the odor arena against another. One way to overcome this problem is to alternate trials rewarding the mouse for navigating toward the left and right lanes. A critical step for checking the plume is to keep the PID needle aligned with the odor source to detect the plume's path. A crucial step in miniscope recording a freely moving mouse is to ensure that the mini-coax wire does not tangle during the task, which can be prevented with a commutator. Helium balloons can be used to prevent the mini-coax wire from coming in front of the mouse. It is critical for the data pre-processing to synchronize the TTL pulses of the FLIR top camera of the odor arena and the miniscope camera. For the EXTRACT procedure, we recommend using non-negative processing to extract the ROIs and dF/F signals better. EXTRACT yields a visual inspection of the traces for each ROI to exclude bad ones. It is critical to decode the X and Y positions of the mouse from the ROIs to have a large dataset with hundreds of epochs for better training the artificial neural network.

The significance of this freely moving recording method with respect to existing head-fixed methods is studying the mouse behavior in an ethologically relevant context with the proper head movement for navigating a complex odor plume. This method is applicable to investigate the dynamic role of dCA1 neurons in complex odorant navigation. Furthermore, the method is not restricted to hippocampus or olfaction. Other potential applications of the technique include studying the role of different brain areas and sensory modalities, including possible applications in visual navigation by using LEDs to indicate the rewarded lanes. In addition, this method is potentially used in real-time closed-loop experiments in which neural calcium from population activity is decoded to trigger neurostimulation or sensory feedback [22–25].

ACKNOWLEDGMENTS:

This research was supported by the US National Institutes of Health (NIH UF1 NS116241 and NIH R01 DC000566), and the National Science Foundation (NSF BCS-1926676). The authors thank Andrew Scallon for helping setting up the Odor Arena chamber.

DISCLOSURES:

The authors declare no conflict of interest.

REFERENCES:

1. Adoff, M.D., Climer, J.R., Davoudi, H., Marvin, J.S., Looger, L.L., Dombeck, D.A. The functional

organization of excitatory synaptic input to place cells. *Nature Communications*. **12** (1), 3558, doi: 10.1038/s41467-021-23829-y (2021).

2. Radvansky, B.A., Oh, J.Y., Climer, J.R., Dombeck, D.A. Behavior determines the hippocampal spatial mapping of a multisensory environment. *Cell Reports*. **36** (5), 109444, doi: 10.1016/j.celrep.2021.109444 (2021).
3. Lewis, S.M. *et al*. Plume Dynamics Structure the Spatiotemporal Activity of Mitral/Tufted Cell Networks in the Mouse Olfactory Bulb. *Frontiers in Cellular Neuroscience*. **15**, 633757, doi: 10.3389/fncel.2021.633757 (2021).
4. Findley, T.M. *et al*. Sniff-synchronized, gradient-guided olfactory search by freely moving mice. *eLife*. **10**, e58523, doi: 10.7554/eLife.58523 (2021).
5. Gire, D.H., Kapoor, V., Arrighi-Allisan, A., Seminara, A., Murthy, V.N. Mice Develop Efficient Strategies for Foraging and Navigation Using Complex Natural Stimuli. *Current Biology*. **26** (10), 1261–1273, doi: 10.1016/j.cub.2016.03.040 (2016).
6. Liu, A., Papale, A.E., Hengenius, J., Patel, K., Ermentrout, B., Urban, N.N. Mouse Navigation Strategies for Odor Source Localization. *Frontiers in Neuroscience*. **14**, 218, doi: 10.3389/fnins.2020.00218 (2020).
7. Tariq, M.F. *et al*. Using Head-Mounted Ethanol Sensors to Monitor Olfactory Information and Determine Behavioral Changes Associated with Ethanol-Plume Contact during Mouse Odor-Guided Navigation. *eneuro*. **8** (1), ENEURO.0285-20.2020, doi: 10.1523/ENEURO.0285-20.2020 (2021).
8. Rigolli, N., Reddy, G., Seminara, A., Vergassola, M. Alternation emerges as a multi-modal strategy for turbulent odor navigation. *eLife*. **11**, e76989, doi: 10.7554/eLife.76989 (2022).
9. Ma, M. *et al*. Sequential activity of CA1 hippocampal cells constitutes a temporal memory map for associative learning in mice. *Current Biology*. S0960982224000216, doi: 10.1016/j.cub.2024.01.021 (2024).
10. Aharoni, D., Khakh, B.S., Silva, A.J., Golshani, P. All the light that we can see: a new era in miniaturized microscopy. *Nature Methods*. **16** (1), 11–13, doi: 10.1038/s41592-018-0266-x (2019).
11. Aharoni, D., Hoogland, T.M. Circuit Investigations With Open-Source Miniaturized Microscopes: Past, Present and Future. *Frontiers in Cellular Neuroscience*. **13**, 141, doi: 10.3389/fncel.2019.00141 (2019).
12. Flusberg, B.A. *et al*. High-speed, miniaturized fluorescence microscopy in freely moving mice. *Nature Methods*. **5** (11), 935–938, doi: 10.1038/nmeth.1256 (2008).
13. Connor, E.G., McHugh, M.K., Crimaldi, J.P. Quantification of airborne odor plumes using planar laser-induced fluorescence. *Experiments in Fluids*. **59** (9), 137, doi: 10.1007/s00348-018-2591-3 (2018).
14. Gumaste, A. *et al*. A Comparison between Mouse, In Silico, and Robot Odor Plume Navigation Reveals Advantages of Mouse Odor Tracking. *eNeuro*. **7** (1), ENEURO.0212-19.2019, doi: 10.1523/ENEURO.0212-19.2019 (2020).
15. Dana, H. *et al*. Thy1-GCaMP6 Transgenic Mice for Neuronal Population Imaging In Vivo. *PLoS ONE*. **9** (9), e108697, doi: 10.1371/journal.pone.0108697 (2014).
16. Thapa, R., Liang, B., Liu, R., Li, Y. Stereotaxic Viral Injection and Gradient-Index Lens Implantation for Deep Brain In Vivo Calcium Imaging. *Journal of Visualized Experiments*. (176), 63049, doi: 10.3791/63049 (2021).

17. Hsiao, Y.-T., Wang, A.Y.-C., Lee, T.-Y., Chang, C.-Y. Using Baseplating and a Miniscope Preanchored with an Objective Lens for Calcium Transient Research in Mice. *Journal of Visualized Experiments*. (172), 62611, doi: 10.3791/62611 (2021).
18. Zhang, L. *et al*. Miniscope GRIN Lens System for Calcium Imaging of Neuronal Activity from Deep Brain Structures in Behaving Animals. *Current Protocols in Neuroscience*. **86** (1), e56, doi: 10.1002/cpns.56 (2019).
19. Pnevmatikakis, E.A., Giovannucci, A. NoRMCorre: An online algorithm for piecewise rigid motion correction of calcium imaging data. *Journal of Neuroscience Methods*. **291**, 83–94, doi: 10.1016/j.jneumeth.2017.07.031 (2017).
20. Inan, H. *et al*. *Fast and statistically robust cell extraction from large-scale neural calcium imaging datasets*. doi: 10.1101/2021.03.24.436279. Neuroscience. (2021).
21. Segalin, C. *et al*. The Mouse Action Recognition System (MARS) software pipeline for automated analysis of social behaviors in mice. *eLife*. **10**, e63720, doi: 10.7554/eLife.63720 (2021).
22. Chen, Z. *et al*. A hardware system for real-time decoding of in vivo calcium imaging data. *eLife*. **12**, e78344, doi: 10.7554/eLife.78344 (2023).
23. Xue, F. *et al*. Multi-region calcium imaging in freely behaving mice with ultra-compact head-mounted fluorescence microscopes. *National Science Review*. **11** (1), nwad294, doi: 10.1093/nsr/nwad294 (2024).
24. Tabourin, L., Bretzner, F., Galstian, T. Towards a mini-endoscope design with spatially selective excitation and imaging. *Biomedical Optics Express*. **15** (3), 1750–1760, doi: 10.1364/BOE.512124 (2024).
25. Mizuta, K., Sato, M. Multiphoton imaging of hippocampal neural circuits: techniques and biological insights into region-, cell-type-, and pathway-specific functions. *Neurophotonics*. **11** (3), 033406, doi: 10.1117/1.NPh.11.3.033406 (2024).

Fig. 1.

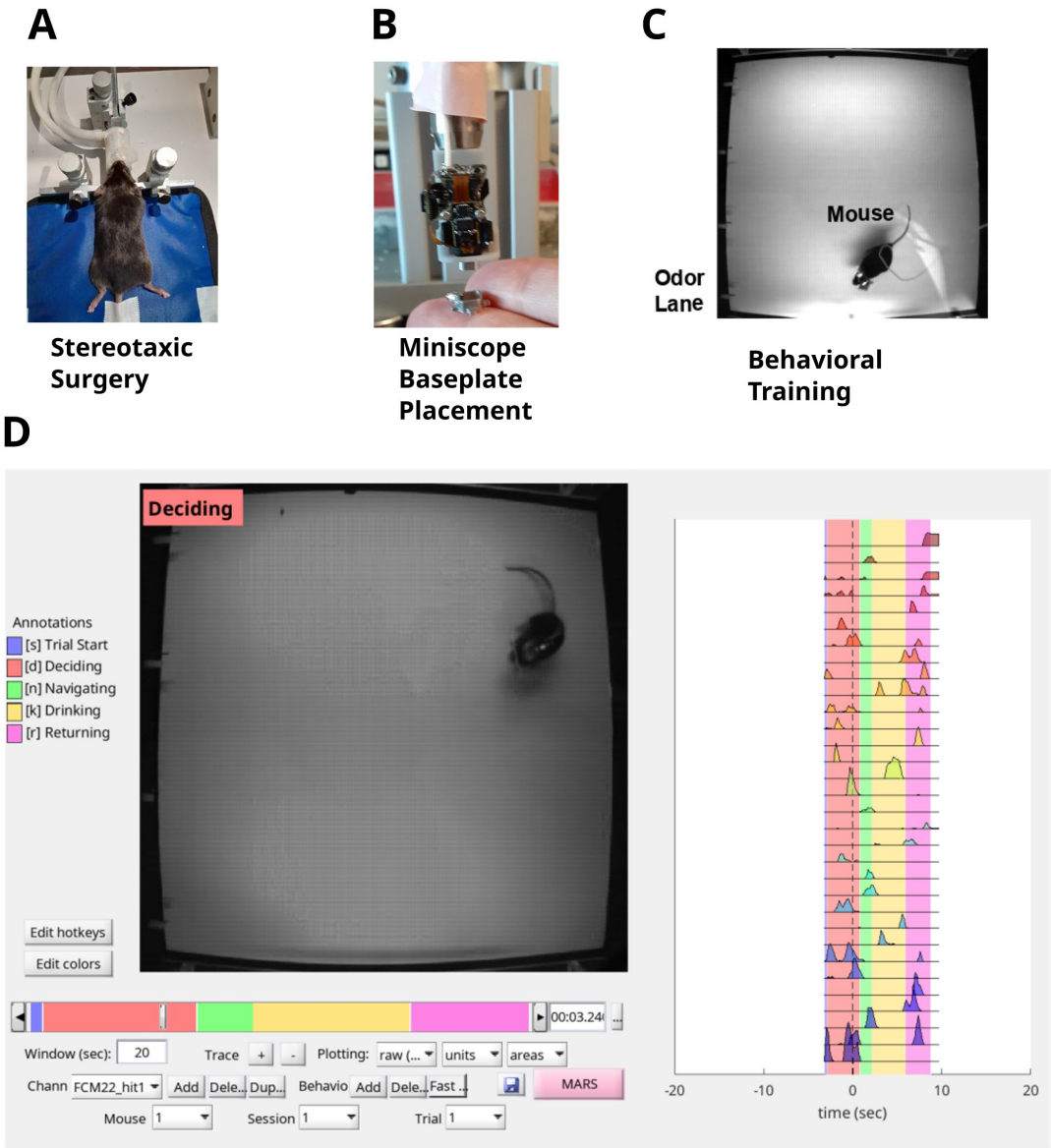

Freely Moving Recording

Fig 2.

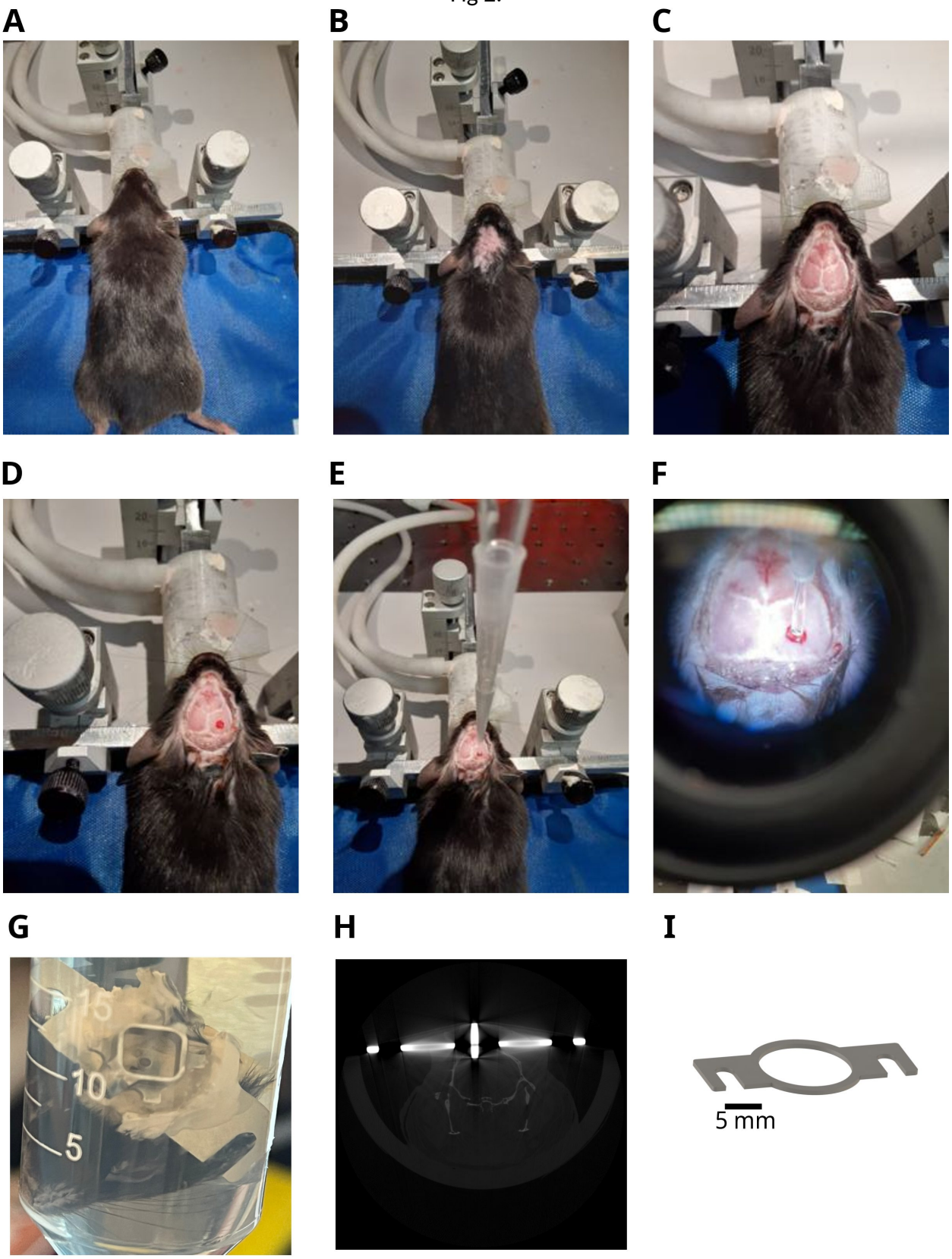

Fig. 3.

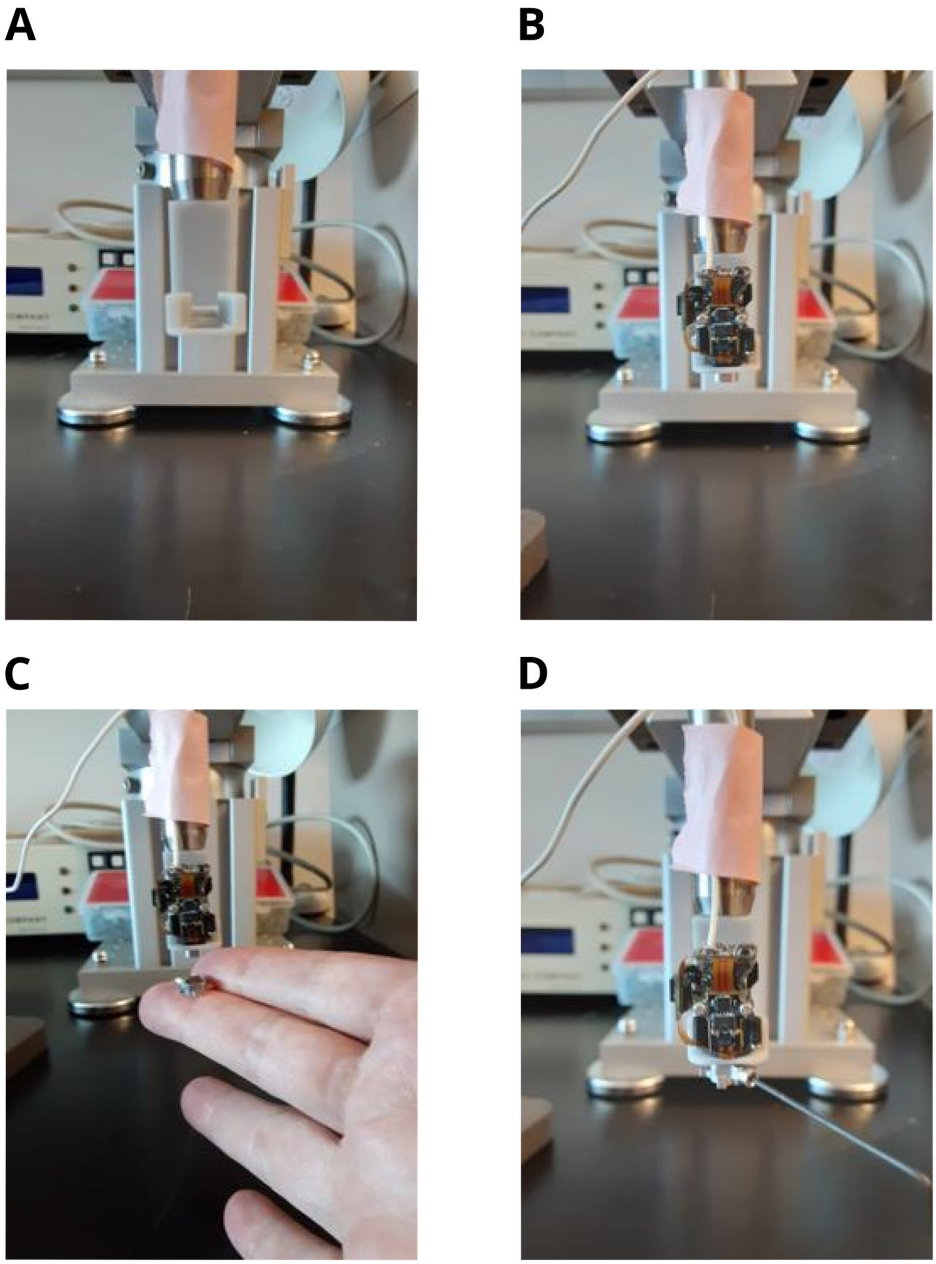

Fig. 4.

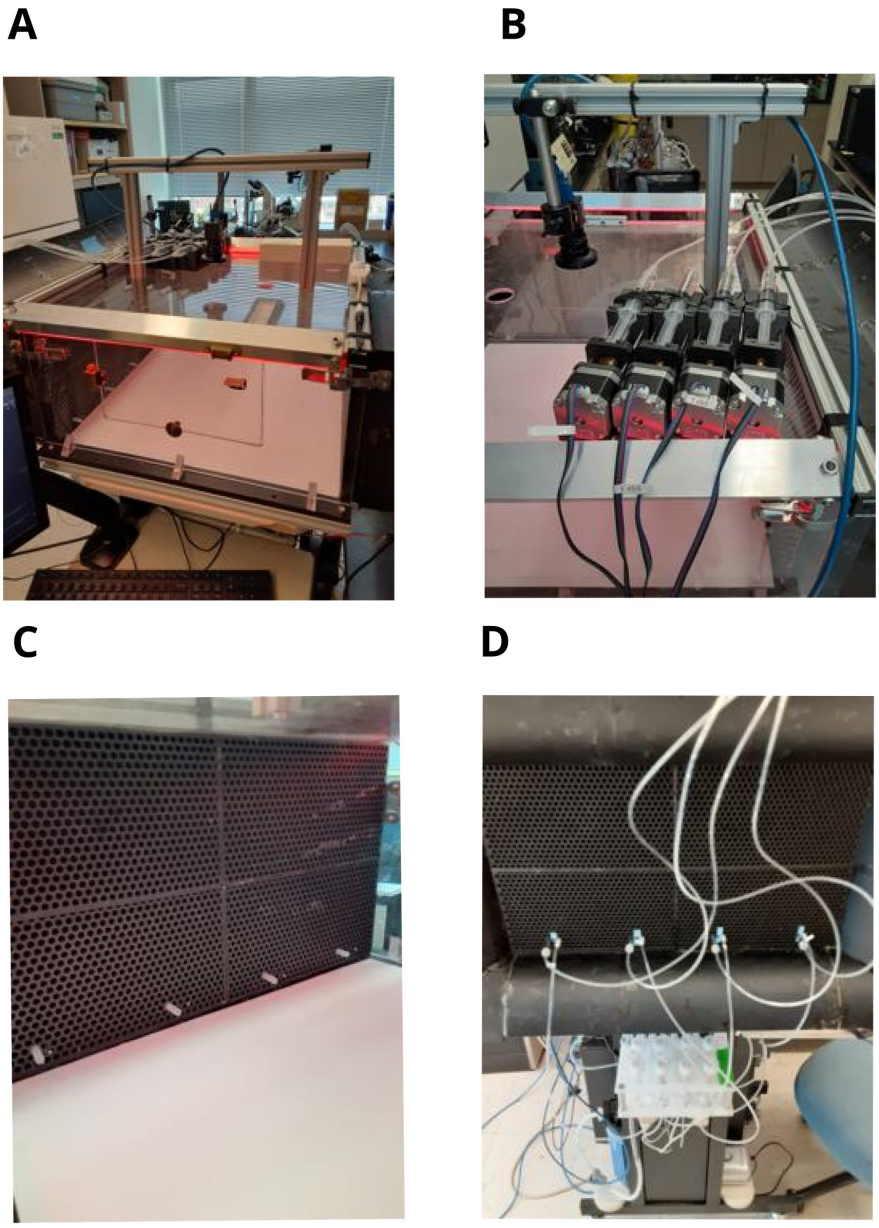

Fig 5.

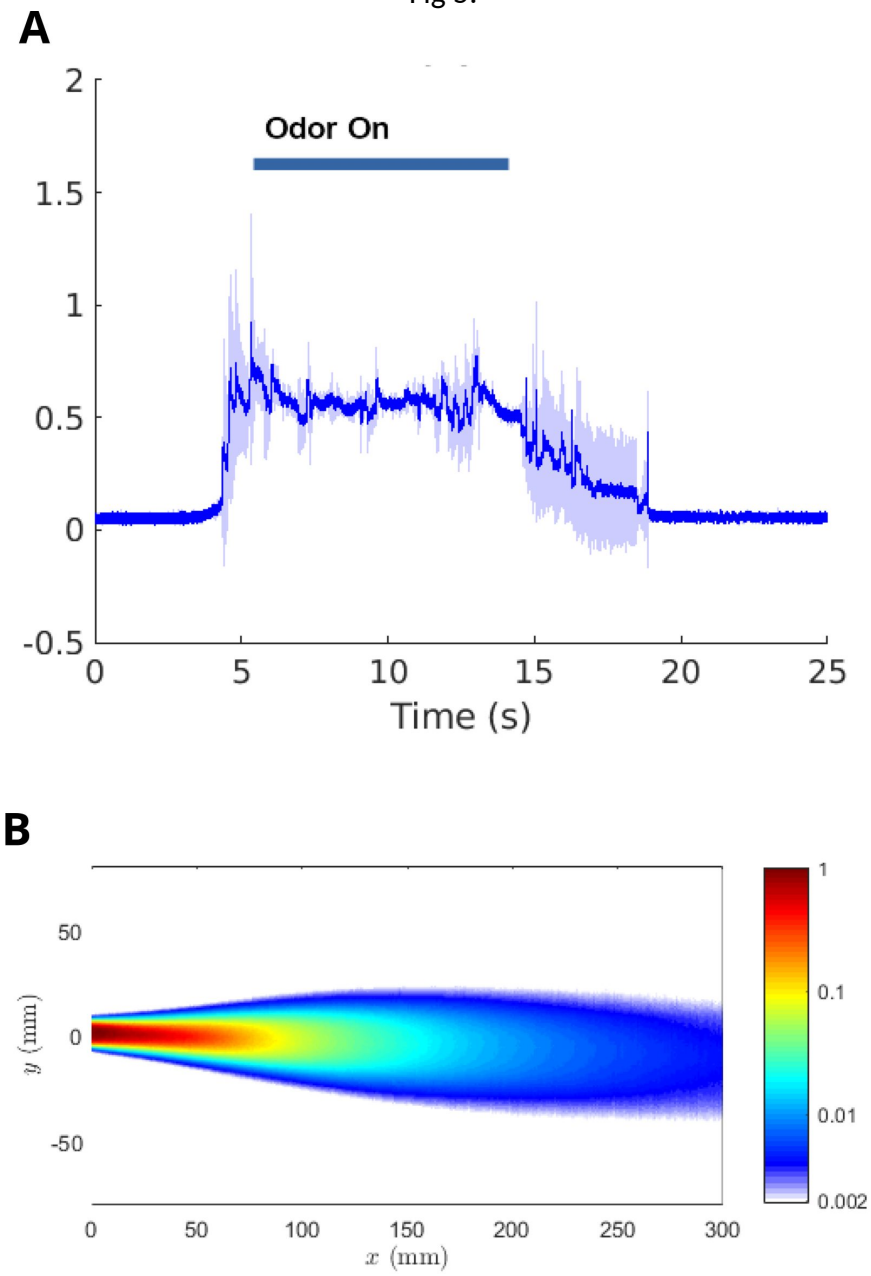
A
Odor On
2
1.5
1
0.5
0
-0.5
0
5
10
15
20
25
Time (s)
B
50
0
-50
y (mm)
0
50
100
150
200
250
300
x (mm)
1
0.1
0.01
0.002

Fig 6.

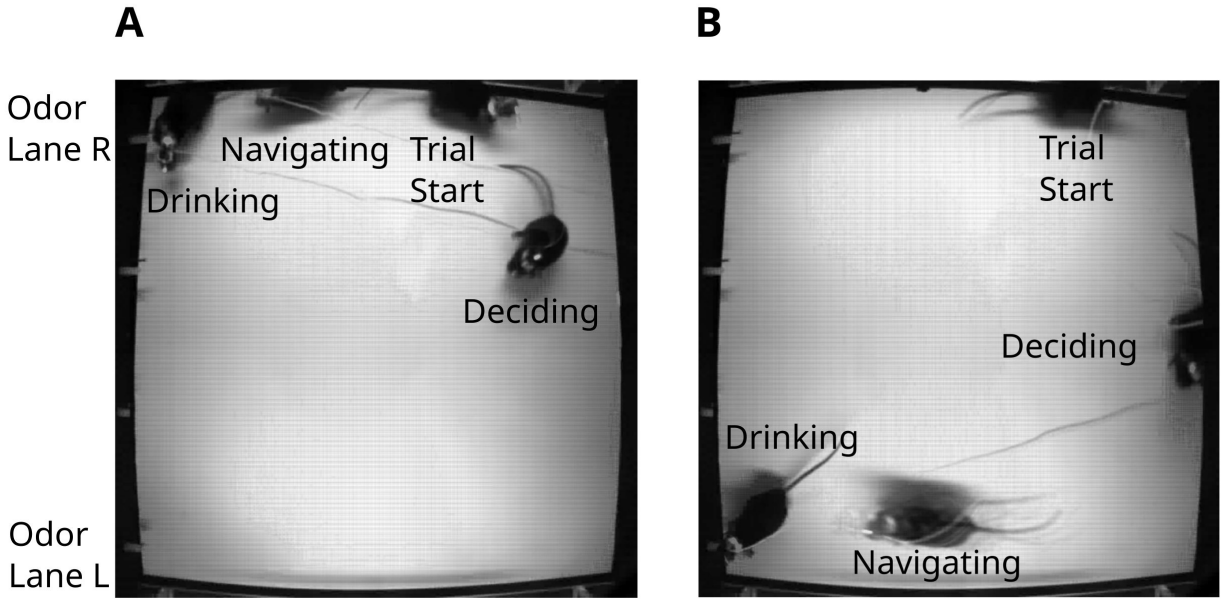
A
B
Odor
Lane R
Navigating
Trial
Start
Drinking
Deciding
Odor
Lane L
Trial
Start
Deciding
Drinking
Navigating

Fig. 7.

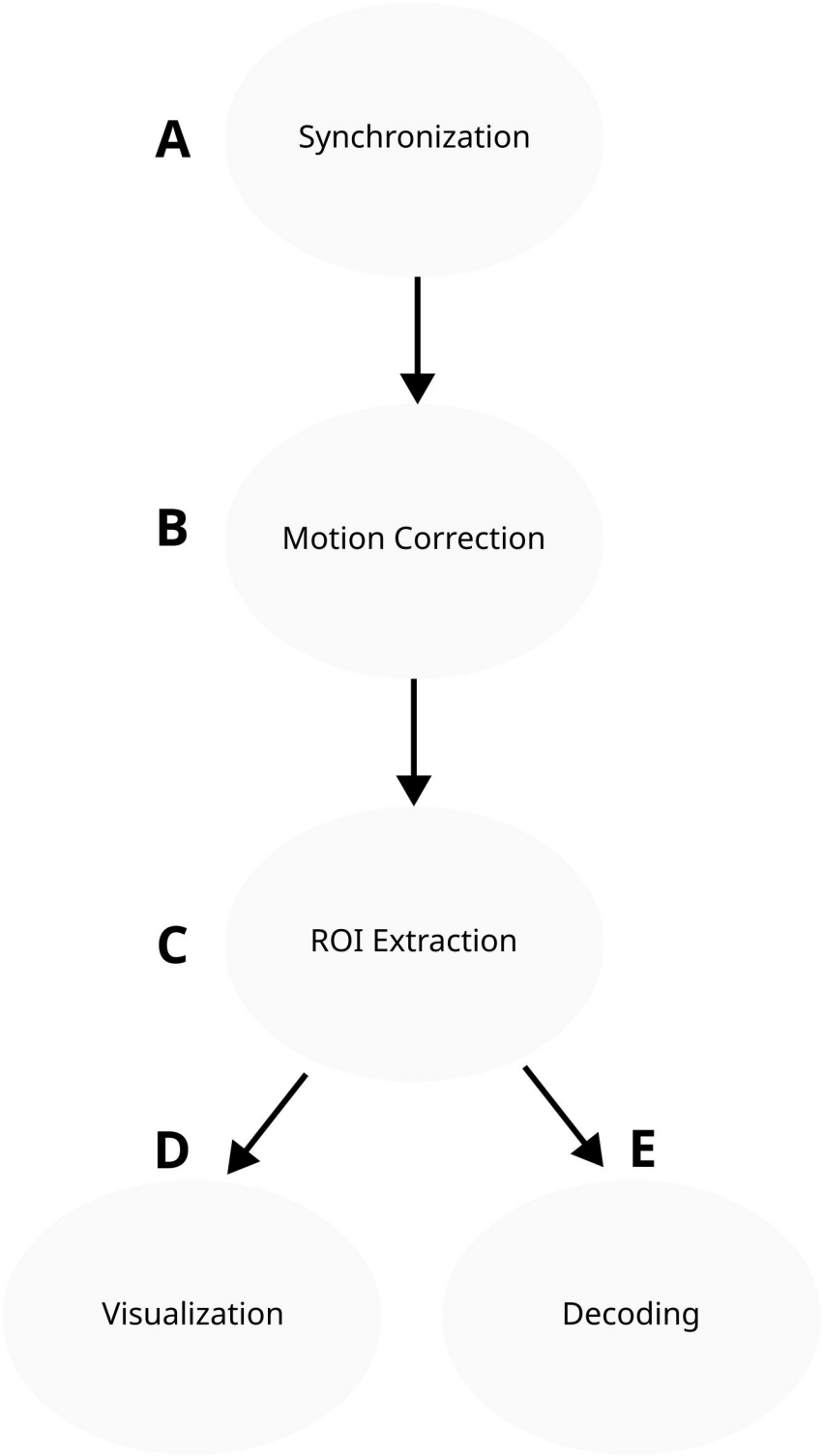
A
Synchronization
B
Motion Correction
C
ROI Extraction
D
E
Visualization
Decoding

Fig. 8.

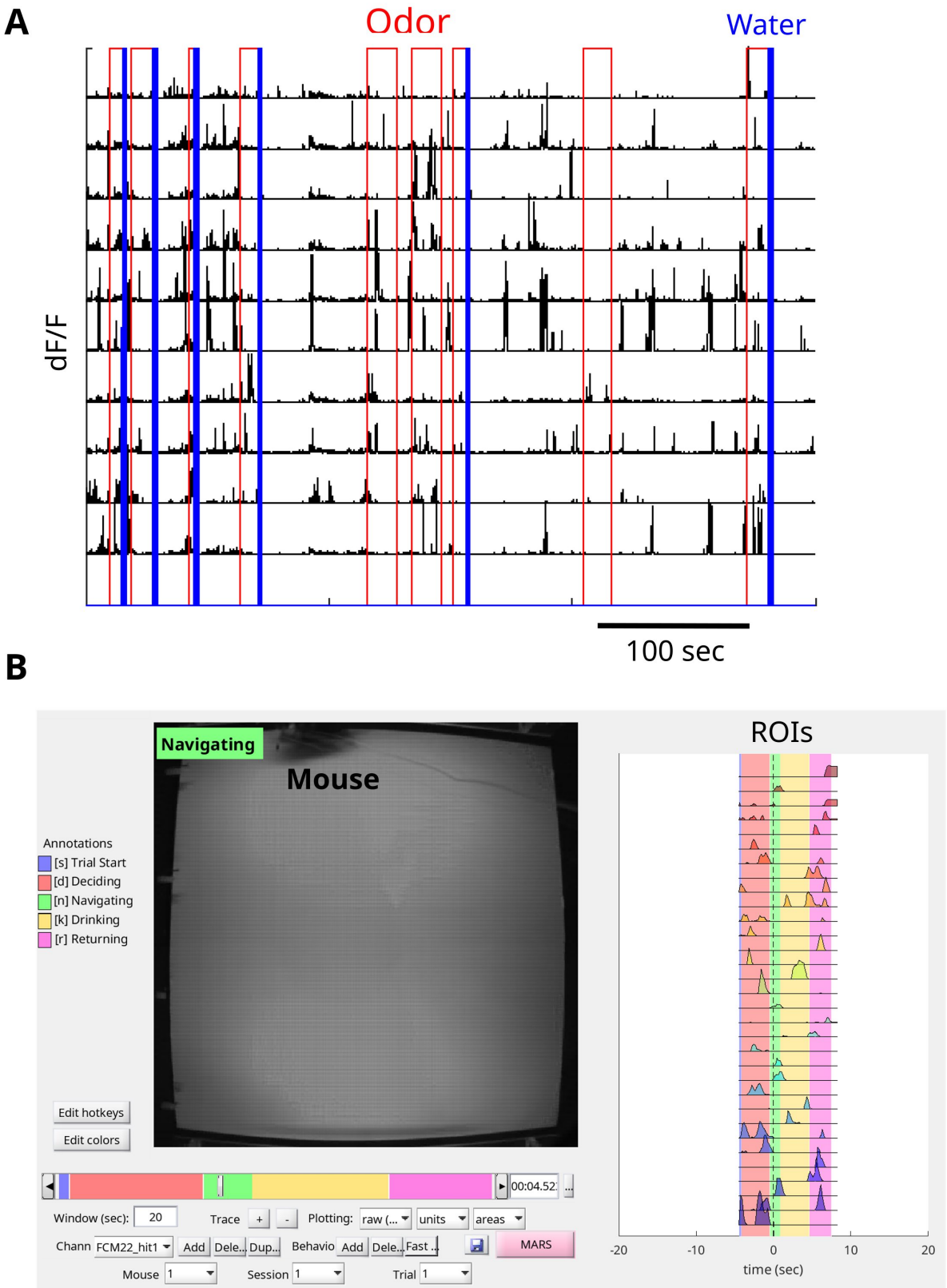
A
Odor
Water
dF/F
100 sec
B
Navigating
Mouse
Annotations
[s] Trial Start
[d] Deciding
[n] Navigating
[k] Drinking
[r] Returning
Edit hotkeys
Edit colors
00:04.52
Window (sec): 20
Trace
Plotting:
raw (...
units
areas
Chann
FCM22_hit1
Add
Dele...
Dup...
Behavio
Add
Dele...
Fast ...
MARS
Mouse
1
Session
1
Trial
1
ROIs
-20
-10
0
10
20
time (sec)

Fig 9.

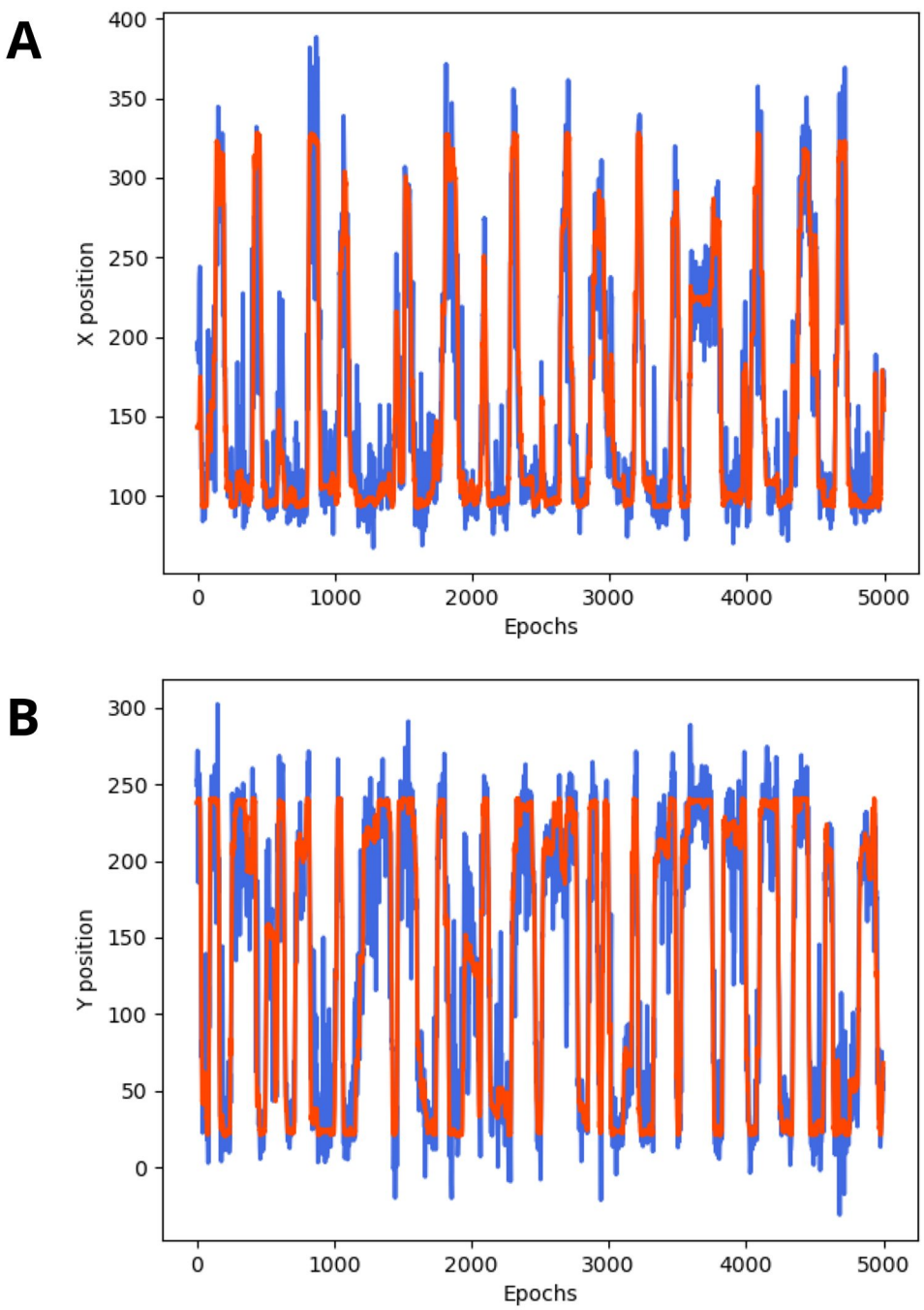
A
400
350
300
250
200
150
100
X position
0
1000
2000
3000
4000
5000
Epochs
B
300
250
200
150
100
50
0
Y position
0
1000
2000
3000
4000
5000
Epochs